ER localized bestrophin1 activates Ca^{2+} dependent ion channels TMEM16A and SK4

René Barro-Soria[1#], Fadi Aldehni[1#], Joana Almaça[1],

Jiraporn Ousingsawat[1], Ralph Witzgall[2], Rainer Schreiber[1], Karl Kunzelmann[1*]

Institut für Physiologie[1] and Anatomie[2] of the Universität Regensburg, Universitätsstraße 31, D-93053 Regensburg

[*]To whom correspondence should be addressed

Tel.: +49 (0)941 943 4302, Fax: +49 (0)941 943 4315,

e-mail: Karl.Kunzelmann@vkl.uni-regensburg.de

[#] RBS and FA contributed equally to the present study

Running Title: Bestrophin 1 activates Ca^{2+} dependent Cl^- channels

Key words: bestrophin, Ca^{2+} activated Cl^- currents, CaCC, Ca^{2+} activated K^+ currents, SK4, TMEM16A, Pak2, purinergic receptors, endoplasmic reticulum, ER, Ca^{2+} store

Abbreviations: hBest1, human bestrophin 1; CaCC, Ca^{2+} activated Cl^- channels; SK4, mall conductance calcium-activated potassium channel type 4; TMEM16A, transmembrane protein 16A; ANO1, anoctamin 1; Pak2, p21-activated protein kinase; ER, endoplasmic reticulum; SERCA, sarcoendoplasmic reticulum calcium ATPase; Stim1, stromal interacting molecule 1; DIDS, 4,4'-diisothio-cyanostilbene-2,2'-disulfonic acid.

Bestrophins form Ca^{2+} activated Cl^- channels and regulate intercellular Ca^{2+} signaling[1]. We demonstrate that bestrophin 1 is localized in the endoplasmic reticulum (ER), where it physically interacts with stromal interacting molecule 1 (Stim1), the ER-Ca^{2+} sensor[2,3]. Intracellular Ca^{2+} transients in HEK293 cells elicited by stimulation of purinergic $P2Y_2$-receptors were augmented but more transient after expression of hBest1, in contrast to dominant negative hBest1-R218C, which attenuated Ca^{2+} increase. The p21-activated protein kinase Pak2 was found to phosphorylate hBest1, thereby enhancing Ca^{2+} signaling and activation of Ca^{2+} dependent Cl^- (TMEM16A)[4] and K^+ (SK4)[5] channels. Lack of bestrophin 1 expression in respiratory epithelial cells of mBest1 knockout mice caused expansion of ER cisterns and induced Ca^{2+} deposits. We propose that hBest1 is important for Ca^{2+} handling of the ER store, probably by controlling the function of Stim1 and by acting as a counter-ion channel to balance transient membrane potentials occurring through inositol trisphosphate (IP_3) induced Ca^{2+} release and refill of the ER-Ca^{2+} store. Thus bestrophin 1 controls activation of Ca^{2+} dependent ion channels by regulation of compartmentalized Ca^{2+} signaling.

Compelling evidence has been provided that bestrophins are Ca^{2+} activated and DIDS-sensitive Cl^- channels (CaCC)[6,7], but much controversy exists about the question whether these proteins indeed form apical Cl^- channels in epithelial cells[8]. Although it has been shown that hBest1 enables Ca^{2+} dependent Cl^- secretion in epithelial cells and that Ca^{2+} dependent Cl^- secretion is reduced in airways of knockout animals[9,10], the precise role of bestrophin for CaCC remains illusive. Surprisingly hBest1 also regulates voltage-gated Ca^{2+} channels[11], which prompted us to search for a link between receptor induced increase of cytosolic Ca^{2+}, bestrophin 1 and CaCC. We found that hBest1 expressed in HEK293 cells co-localizes with ER markers such as calnexin, Stim1 (Fig. 1a) or calreticulin (see Supplementary information,

Fig. S1a online). hBest1 was coimmunoprecipitated with Stim1 (Fig. 1b), but not with other proteins involved in ER-Ca^{2+} signaling such as IP_3-receptors, the Ca^{2+}-ATPase SERCA or components of the store operated Ca^{2+} influx (SOCE) pathway such as TRPC1 (see Supplementary information, Fig. S1b online). Localization of hBest1 in the ER and physical interaction with Stim1 predicts a role of hBest1 for intracellular Ca^{2+} signaling.

We measured the intracellular Ca^{2+} concentration $[Ca^{2+}]_i$ in hBest1 transfected HEK293 cells, using Fura2 as Ca^{2+}-senstive dye and we found that hBest1 largely augments Ca^{2+} signals induced by stimulation of purinergic receptors with ATP (100 μM) (Fig. 1c). In the presence of hBest1, ATP caused a fast and transient Ca^{2+} peak that quickly recovered to a plateau (Fig. 1d,e). Using the membrane bound fluorescence dye FFP-18 we found that the Ca^{2+} plateau was reduced after overexpression of hBest1, but was extended in cells overexpressing the bestrophin 1 mutant hBest1-R218C (Fig. 1f). Since this was also observed in the absence of extracellular Ca^{2+} (Fig. 1g), it suggests reduced reuptake of $[Ca^{2+}]_i$ into the ER in hBest1-R218C expressing cells (Fig. 1h). The R218C mutation is known to abolish ion channel function of bestrophin 1 and to cause an autosomal inherited form of macular dystrophy of the retina[1]. Since bestrophins exist at least as dimeric proteins[12], we assume hBest1-R218C would act as a dominant negative mutant on hBest1 expressed endogenously in HEK293 cells. In fact HEK293 cells expressed low but detectable levels of hBest1 as demonstrated by RT-PCR and Western blotting, and expression was suppressed by siRNA (see Supplementary information, Fig. S1c online). Moreover in the absence of extracellular Ca^{2+}, store release by inhibition of the SERCA-pump with cyclopiazonic acid (CPA) was reduced upon expression of hBest1-R218C, confirming the role of Best1 for Ca^{2+} release from the store (Fig. 1i,j). We fused the Ca^{2+} sensitive protein G-CaMP2[13] to hBest1 and to hBest1-R218C, respectively, to measure $[Ca^{2+}]_i$ in close proximity of bestrophin and near the external ER membrane. Using these constructs as Ca^{2+} probes, oscillations of $[Ca^{2+}]_i$ were observed upon stimulation with

ATP that were longer lasting but of lower amplitude for hbest1-R218C-G-CaMP2 (n = 4.9 ± 0.4) than for hbest1-G-CaMP2 (n = 7.9 ± 0.5; n = 12, $p<0.05$) expressing cells (Fig. 1k,l). Thus hBest1 facilitates Ca^{2+} release from the ER and was well as reuptake by the SERCA pump, probably by acting as a counter-ion channel to balance transient negative potentials generated by Ca^{2+} release and reuptake. Notably the existence of an ATP activated, DIDS-sensitive 64 kDa Cl^- channel in the ER has been described earlier[14]. In the sarcoplasmic reticulum Cl^- channels have long been proposed to play an essential role in excitation-contraction coupling by balancing charge movement during calcium release and uptake[15,16].

To understand the role of bestrophin for Ca^{2+}signaling and activation of Ca^{2+} dependent ion channels, we searched for additional partner proteins. Immunoprecipitation of hBest1 from HEK293 cells and 2D-PAGE followed by MALDI-TOF analysis identified the p21 activated serine/threonine kinase Pak2 as a novel binding partner of hBest1 (see Supplementary information, Fig. S1d online). Pak2 is activated by autophosphorylation through binding of small G proteins such as Cdc42 and Rac1. It is transiently activated under cell stress and by phosphatidylinositol 3-kinase or tyrosine kinase, or becomes permanently activated through cleavage by caspase-3[17,18]. hBest1 carries a strong consensus sequence for Pak2 in the C-terminus and was *in vitro* phosphorylated by hPak2, while phosphorylation was eliminated by mutation of the responsible serine 358 to alanine (Fig. 1m). Pak2 phosphorylation and translocation to the ER may lead to proliferation or cytostasis/autophagy[17,18]. We examined the functional impact of Pak2 on endogenous xBest1[19] and activation of Ca^{2+} dependent Cl^- channels, by expression of $P2Y_2$ receptors in *Xenopus* oocytes and stimulation with ATP. Oocytes were either injected with Pak2 enzyme or with an equal volume of H_2O (Fig. 2a). Activation of whole cell Cl^- currents by ATP and increase in $[Ca^{2+}]_i$ was largely enhanced in Pak2-injected oocytes, which was suppressed when extracellular Cl^- was replaced by impermeable gluconate (Fig. 2b). Notably, Pak2 injection also augmented a delayed inward

current activated by ATP. This current inhibited by removal of Na^+ and Ca^{2+} from the extracellular bath solution (Fig. 2a,c). Thus, Pak2 augments endogenous CaCC as well as Ca^{2+} influx into receptor activated *Xenopus* oocytes, probably by augmenting Ca^{2+} release from the store and activation of store operated Ca^{2+} influx. Activation of CaCC by stimulation of endogenous receptors for lysophosphatidic acid was also enhanced by Pak2-injection, while receptor independent activation of CaCC by ionomycin was unaffected by Pak2 (see Supplementary information, Fig. S2b online). Moreover, in contrast to Pak2 injection of Pak1 did neither augment CaCC nor ATP induced inward currents (see Supplementary information, Fig. S2c,d online). A previous report indicated that bestrophin 1 interacts physically and functionally with protein phosphatase 2A (PP2A)[20]. We speculated that Pak2-phosphorylated Best1 is rapidly dephosphorylated and deactivated by PP2A[21]. In fact in the presence of the PP2A-inhibitor okadaic acid (OKA; 100 nM), ATP activated whole cell conductance (G_{ATP}) was augmented to the same level as after injection of Pak2 (Fig. 2d). In contrast, expression of dominant negative hBest-R218C reduced G_{ATP} in oocytes and abrogated the stimulating effect of Pak2 (Fig. 2d). Notably activation of CaCC by ER-store depletion through inhibition of SERCA by CPA, was also augmented after injection of Pak2 (Fig. 2e,f). We conclude that activation of xBest by Pak2 improves Cl^- counter-ion movement thereby facilitating receptor operated Ca^{2+} signaling and activation of endogenous CaCC.

Improved Ca^{2+} signaling by activation of bestrophin 1 may also enhance activation of other Ca^{2+} dependent ion channels such as the Ca^{2+} activated K^+ channel SK4[5]. We therefore expressed $P2Y_2$ receptors together with hSK4 in *Xenopus* oocytes. The membrane voltage of these oocytes was strongly hyperpolarized and further hyperpolarized to E_{K+} upon stimulation with ATP and activation of hSK4 (Fig. 2g). Activation of CaCC was negligible in hSK4 expressing oocytes, as indicated by the fact that removal of extracellular Cl^- (5 Cl^-) did not compromise ATP activated conductance, while 5 mM Ba^{2+} abolished activation of a whole

cell conductance by ATP (see Supplementary information, Fig. S2f online). Moreover, the CaCC-inhibitor DIDS did not inhibit ATP-activated conductance (-DIDS: 18.3 ± 2.1 vs. +DIDS: 17.3 ± 1.9 μS; n = 17), while the SK4-inhibitor TRAM-34 inhibited the effect of ATP significantly (-TRAM-34: 18.3 ± 2.1 vs. +TRAM-34: 6.43 ± 1.5 μS; n = 12). hSK4-K^+ currents were activated either through stimulation of purinergic receptors by ATP or by directly increasing $[Ca^{2+}]_i$ using ionomycin (Fig. 2h). Similar to endogenous TMEM16A currents, also receptor-activated hSK4-currents were augmented by Pak2, while activation through a direct increase of $[Ca^{2+}]_i$ with ionomycin, was not affected by Pak2 (Fig. 2h;i). Furthermore, activation of hSK4 by ATP was attenuated when hBest1-R218C was coexpressed and in these oocytes injection of Pak2 did not augment hSK4 currents (Fig. 3a,b). Taken together these results indicate an essential role of *Xenopus* bestrophin and Pak2 in receptor mediated activation of overexpressed hSK4 channels, and endogenous Ca^{2+} dependent Cl^- channels, which have been recently identified as xTMEM16A[4,22].

A fraction of hBest1 overexpressed in HEK293 cells reaches the cell membrane, where it generates a Ca^{2+} activated Cl^- current[6,7,23]. Regulation of bestrophin Cl^- currents by Pak2 was further examined in whole cell patch clamp experiments with HEK293 cells, coexpressing hPak2 with either hBest1 or hBest1-R218C, or coinjected with siRNA-hBest1 (Fig. 3c). ATP activated bestrophin Cl^- currents in hPak2/hBest1 transfected cells, as indicated by a current increase that was inhibited by reducing bath Cl^- concentration (30Cl, grey bar). In contrast, both dominant negative hBest1-R218C and siRNA-hBest1 significantly inhibited current activation by ATP, demonstrating a direct activation of bestrophin Cl^- currents by Pak2 (Fig. 3c,d). Human airway epithelial cells, such as 16HBE14o- express both hBest1, hSK4 and hTMEM16A endogenously[9,24]. We demonstrated the importance of endogenous Pak2 for receptor-mediated activation of Cl^- (hTMEM16A) and K^+ (hSK4) currents in human airway

epithelial cells (16HBE) by knockdown of Pak2-expression using three independent batches of siRNA (Fig. 3e).

Membrane localized TMEM16A proteins are likely to resemble the molecular counterpart of the ubiquitous Ca^{2+} activated Cl^- channel[4,22,24]. We directly demonstrate that ER-localized hBest1 Cl^- channels support receptor-activation of TMEM16A channels in the plasma membrane by overexpressing both proteins in HEK293 cells. Overexpression of TMEM16A only produced large ATP-activated whole cell currents that were further augmented upon coexpression of hBest1 (Fig. 3f). In contrast TMEM16A-currents were reduced by coexpression of dominant negative hBest1-R218C, probably by interfering with receptor mediated store release (Fig. 3g). The concept of counter-ion movement for Ca^{2+}-release from the ER has been demonstrated recently for TRIC K^+ channels[25,26]. Cardiomyocytes of mice lacking expression of TRIC demonstrate remarkable suppression of ER-dependent Ca^{2+} signaling and present embryonic cardiac lethality beyond E10.5[26]. Electron microscopy revealed extensively swollen SR/ER structures in cardiomyocytes of TRIC KO-mice and showed frequent electron-dense Ca^{2+}-oxalate deposits in the bloated SR/ER. Using electron microscopy we examined tracheal epithelial cells of mBest1-/- mice, which were shows to express attenuated Ca^{2+}-activated Cl^- currents[10]. In striking similarity to the changes observed in TRIC KO-animals, we also detected bloated ER structures in airway epithelial cells of Best1-/- mice (Fig. 4a). Moreover, using an oxalate-substituted fixative solution, we detected electron-dense Ca^{2+} precipitations in the ER of Best1-/- mice. Similar structures were occasionally found in cells from wt animals, but did not contain Ca^{2+} (Fig. 4b). We conclude that bestrophin 1 operates as a counter ion channel to control Ca^{2+} filling of the ER, thereby facilitating activation of Ca^{2+} dependent hSK4 and TMEM16A channels. Bestrophin operates in conjunction with other proteins that are essential for receptor-coupled Ca^{2+} signaling such as Stim1 and maybe components of the store operated Ca^{2+} entry[27,28].

Acknowledgments

DFG SFB699 A6/A7, DFG KU 756/8-2 and Else Kröner-Fresenius-Stiftung P36/05//A44/05. We are grateful for the technical expertise of Christine Meese, Karin Schadendorf, Helga Schmidt and Uwe de Vries in performing the ultrastructural analysis. The Ca^{2+} sensitive GFP protein G-CaMP2 was kindly provided by Dr. J. Nakai, Wako City Saitama, Japan. We gratefully acknowledge the supply of the vmd2-/- mice by MERCK Research Laboratories, 770 (Sumneytown Pike West Point, PA, USA).

References

1. Hartzell,H.C. Molecular Physiology of Bestrophins: Multifunctional Membrane Proteins Linked to Best Disease and Other Retinopathies. *Physiological Reviews* **88**, 639-672 (2008).
2. Zhang,S.L. *et al.* STIM1 is a Ca2+ sensor that activates CRAC channels and migrates from the Ca2+ store to the plasma membrane. *Nature.* **437**, 902-905 (2005).
3. Yuan,J.P. *et al.* SOAR and the polybasic STIM1 domains gate and regulate Orai channels. *Nat. Cell Biol.* (2009).
4. Yang,Y.D. *et al.* TMEM16A confers receptor-activated calcium-dependent chloride conductance. *Nature.* (2008).
5. Joiner,W.J., Wang,L.Y., Tang,M.D. & Kaczmarek,L.K. hSK4, a member of a novel subfamily of calcium-activated potassium channels. *Proc. Natl. Acad. Sci. U. S. A.* **94**, 11013-11018 (1997).
6. Qu,Z., Fischmeister,R. & Hartzell,H.C. Mouse bestrophin-2 is a bona fide Cl(-) channel: identification of a residue important in anion binding and conduction. *J Gen Physiol* **123**, 327-340 (2004).
7. Sun,H., Tsunenari,T., Yau,K.W. & Nathans,J. The vitelliform macular dystrophy protein defines a new family of chloride channels. *Proc. Natl. Acad. Sci. U. S. A. 2002 Mar.* **99**, 4008-4013 (2001).
8. Kunzelmann,K., Milenkovic,V.M., Spitzner,M., Barro Soria,R. & Schreiber,R. Calcium dependent chloride conductance in epithelia: Is there a contribution by Bestrophin? *Pflügers Arch* **454**, 879-889 (2007).
9. Barro Soria,R., Spitzner,M., Schreiber,R. & Kunzelmann,K. Bestrophin 1 enables Ca2+ activated Cl- conductance in epithelia. *J Biol Chem* **281**, 17460-17467 (2006).
10. Barro Soria,R., Schreiber,R. & Kunzelmann,K. Bestrophin 1 and 2 are components of the Ca2+ activated Cl- conductance in mouse airways. *BBA* **1783**, 1993-2000 (2008).

11. Rosenthal,R. *et al.* Expression of bestrophin-1, the product of the VMD2 gene, modulates voltage-dependent Ca2+ channels in retinal pigment epithelial cells. *FASEB J* **20**, 178-180 (2005).

12. Stanton,J.B., Goldberg,A.F., Hoppe,G., Marmorstein,L.Y. & Marmorstein,A.D. Hydrodynamic properties of porcine bestrophin-1 in Triton X-100. *Biochim. Biophys. Acta.* **1758**, 241-247 (2006).

13. Nakai,J., Ohkura,M. & Imoto,K. A high signal-to-noise Ca(2+) probe composed of a single green fluorescent protein. *Nat. Biotechnol.* **19**, 137-141 (2001).

14. Begault,B., Anagnostopoulos,T. & Edelman,A. ATP-regulated chloride conductance in endoplasmic reticulum (ER)-enriched pig pancreas microsomes. *Biochim. Biophys Acta.* **1152**, 319-327 (1993).

15. Kourie,J.I. ATP-sensitive voltage- and calcium-dependent chloride channels in sarcoplasmic reticulum vesicles from rabbit skeletal muscle. *J Membr. Biol.* **157**, 39-51 (1997).

16. Coonan,J.R. & Lamb,G.D. Effect of chloride on Ca2+ release from the sarcoplasmic reticulum of mechanically skinned skeletal muscle fibres. *Pflugers Arch.* **435**, 720-730 (1998).

17. Huang,Z., Ling,J. & Traugh,J.A. Localization of p21-activated protein kinase gamma-PAK/Pak2 in the endoplasmic reticulum is required for induction of cytostasis. *J Biol Chem.* **278**, 13101-13109 (2003).

18. Wilkes,M.C., Murphy,S.J., Garamszegi,N. & Leof,E.B. Cell-type-specific activation of PAK2 by transforming growth factor beta independent of Smad2 and Smad3. *Mol Cell Biol.* **23**, 8878-8889 (2003).

19. Qu,Z., Wei,R.W., Mann,W. & Hartzell,H.C. Two bestrophins cloned from Xenopus laevis Oocytes express Ca-activated Cl currents. *J Biol Chem* **278.**, 49563-49572 (2003).

20. Marmorstein,L.Y. *et al.* Bestrophin interacts physically and functionally with protein phosphatase 2A. *J Biol Chem 2002 Aug. 23. ;277. (34.):30591. -7.* **277**, 30591-30597 (2002).

21. Zhan,Q., Ge,Q., Ohira,T., Van Dyke,T. & Badwey,J.A. p21-activated kinase 2 in neutrophils can be regulated by phosphorylation at multiple sites and by a variety of protein phosphatases. *J Immunol.* **171**, 3785-3793 (2003).

22. Schroeder,B.C., Cheng,T., Jan,Y.N. & Jan,L.Y. Expression cloning of TMEM16A as a calcium-activated chloride channel subunit. *Cell.* **134**, 1019-1029 (2008).

23. Milenkovic,V.M., Schreiber,R., Barro Soria,R., AlDehni,F. & Kunzelmann,K. Functional assembly and purinergic activation of bestrophins. *Pflugers Arch (in press)* **.**, (2009).

24. Caputo,A. *et al.* TMEM16A, A Membrane Protein Associated With Calcium-Dependent Chloride Channel Activity. *Science.* **322**, 590-594 (2008).

25. Wood,P.G. & Gillespie,J.I. In permeabilised endothelial cells IP3-induced Ca2+ release is dependent on the cytoplasmic concentration of monovalent cations. *Cardiovasc. Res.* **37**, 263-270 (1998).

26. Yazawa,M. *et al.* TRIC channels are essential for Ca2+ handling in intracellular stores. *Nature.* **448**, 78-82 (2007).

27. Penna,A. *et al.* The CRAC channel consists of a tetramer formed by Stim-induced dimerization of Orai dimers. *Nature.* (2008).

28. Smyth,J.T. *et al.* Emerging perspectives in store-operated Ca2+ entry: roles of Orai, Stim and TRP. *Biochim. Biophys. Acta.* **1763**, 1147-1160 (2006).

29. Bachhuber,T. *et al.* Chloride interference with the epithelial Na+ channel ENaC. *J Biol Chem* **280**, 31587-31594 (2005).

30. Takeshima,H. *et al.* Embryonic lethality and abnormal cardiac myocytes in mice lacking ryanodine receptor type 2. *EMBO J.* **17**, 3309-3316 (1998).

Methods

Cell culture, cDNAs, and transfection: Cell lines from human embryonic kidney (HEK-293) and human bronchial epithelium (16HBE14o-) were cultured as described elsewhere[9]. cDNA for human bestrophin 1 (kindly provided by Dr. J. Nathans; Johns Hopkins University, Baltimore, USA), hStim1 (OriGene Technologies, Rockville, USA), hIP3R-3 (kindly provided by Dr. H. De Smedt, Leuven, Belgium), hTRPC1 (kindly provided by Dr. L. Birnbaumer, Research Triangle Park, USA), hPak2 (kindly provided by Dr. K. Saksela, Tampere, Finland), TMEM16A (cloned from 16HBE14o- cells by RT-PCR), SK4 (kindly provided by Dr. W. J. Joiner, New Haven, USA) and the high Ca^{2+} sensitive GFP protein (G-CaMP2) (kindly provided by Dr. J. Nakai, Wako City Saitama, Japan[13] were cloned into mammalian expression vectors. hBest1 and $P2Y_2$ receptors were His_6-tagged at the C-terminus. Site specific mutations (hBest1-R218C, hBest1-S358A, were introduced using QuickChange™ (Stratagene, Heidelberg, Germany). G-CaMP2 fusion protein were generated by PCR. All cDNAs were verified by sequencing. Cells were transfected using standard methods (lipofectamine, Invitrogen, Karlsruhe, Germany). All experiments were performed 48 hours after the transfection.

Immunocytochemistry: HEK293 cells were grown on glass cover slips and washed three times in PBS. Cells were fixed with methanol at -20°C for 5 min or with 4% paraformaldehye and 0.2 M picric acid in PBS for 10 min and incubated with primary antibodies at 4°C overnight. Polyclonal hBest1 antibodies were raised against mouse best1 (sequence AESYPYRDEAGTKPVLYE) or the human best1 (sequence KDHMDPYWALENRDEAHS) (Davids Biotechnologie, Regensburg, Germany). Mouse monoclonal anti-human calreticulin and mouse monoclonal anti-hSTIM1antibodies were from BD Transduction Laboratories (Heidelberg Germany). Mouse monoclonal anti-human calnexin was raised against amino acid residues 116-301. For immunofluorescence cells were incubated with secondary

AlexaFluro 488 goat anti-rabbit IgG and tetramethylrhodamine goat anti-mouse IgG (Molecular probes) for 1 hr at room temperature and counterstained with Hoe33342 (Sigma-Aldrich, Taufkirchen, Germany). Immunofluorescence was detected using an Axiovert 200 microscope equipped with an ApoTome and Carl Zeiss AxioVision software (Axiovert 200M, Zeiss, Jena, Germany).

Measurement of the intracellular Ca^{2+} concentration:. HEK293 cells were loaded either with 5 µM Fura2-AM or Fura-piperazine-$C_{12}H_{25}$ (FFP-18, TEFLabs, Austin, USA) in Ringer solution at 37°C for 2 h. Fluorescence was detected at 37°C, using an inverted microscope IMT-2 (Olympus, Nürnberg, Germany) and a high speed polychromator system (VisiChrome, Puchheim, Germany). FFP-18 was excited at 340/380 nm and emission was recorded between 470 and 550 nm using a CCD camera (CoolSnap HQ, Visitron). The results were obtained at 340/380 nm fluorescence ratio (after background subtraction). When using hbest1-G-CaMP2 or hbest1-R218C-G-CaMP2, fluorescence was excited at 485nm and was detected at 520 to 550 nm.

2D-Electrophorese and Maldi-Tof Analysis: D-PAGE was performed with IPG strip gels (Amersham, Germany) after rehydration overnight at room temperature. Isoelectric focusing was carried out with an IPGphor (Amersham Biosciences) for a total of 16 kVh at 20 °C. The IPG gel was equilibrated in 3 M urea, 50 mM Tris–HCl pH 8.8, 30% glycerol, 1.0% SDS, and 16 mM DTT for 15 min. Equilibrated IPG gels were placed on the top of the second-dimension 10 % SDS gel with embedding agarose, and second-dimension electrophoresis was performed at room temperature for 5h. Proteins were silver stained and spots were excised, trypsin digested and analyzed by MALDI-TOF and mass spectrometry database comparison (SEQLAB, Goettingen, Germany).

Immunoprecipitation and Western blotting: Protein was isolated from transfected HEK293 cells in lysis buffer containing 50 mM Tris-HCl 150mM NaCl, 50mM Tris, 100mM DTT, 1% NP-40, 0,5 % Deoxicholate sodium, and 1% protease inhibitor cocktail (Sigma, Germany). Prior to addition of 1-5 µg of the primary antibody, protein lysates were pre-cleared with protein A/G agarose beads (Pierce, Rockford, USA). Incubation of the pre-cleared protein lysates with primary antibodies was performed overnight at 4°C and the protein-antibody complex was immobilized with addition of 25 µl of 50 % slurry of protein A/G- or Ni NTA-Agarose beads for 1 hour at 4 °C. The beads were washed three times in lysis buffer and after the last washing step beads were boiled in 1 x Laemmli sample buffer for Western Blot analysis or the proteins were dissolved in 8 M urea, 4% CHAPS, 60 mM DTT, 2% Pharmalyte™ 3–10, 0.002% bromophenol blue for 2D-PAGE analysis. For western Blot analysis, the 10 % SDS polyacrylamide gel and transferred to a PVDF membrane (GE Healthcare Europe GmbH, Munich, Germany) using semi dry transfer (BioRad, Munich, Germany). Membranes were incubated with first antibodies (dilution from 1:2000 to 1:5000) over night at 4°C. Proteins were visualized using a (HRP) conjugated secondary antibody (dilution 1:30000,) and ECL Detection Kit (GE Healthcare, Munich, Germany), the protein bands were detected by FujiFilm LAS-3000.

In vitro phosphorylation: Human Bestrophin C- terminal domains (wt and mutant) were expressed in BL21 (DE3) *E. coli* strain from a plasmid encoding a 295 fragment from position 291 to 585 with an N-terminal polyhistidine (6xHis) tag and SUMO in the pETSUMO™ vector (Invitrogen, Carlsbad, USA). Cells were grown to A600= 0.8-1 at 37ºC and induced with 0.5 mM IPTG for 12–16 h at 16ºC. After production in bacteria, the hBest1-C regions were purified through a Talon Metal Affinity Resin (Clontech Laboratories, Mountain View, USA) and samples were further concentrated and exchanged into the buffer of interest. Purity of the samples was analyzed by SDS-PAGE and western blotting. The C-terminal of hbest1

was phosphorylated by Pak2 (300ng) in 20 µl phosphorylation buffer (25 mM Tris-HCl, pH 7.5, 5 mM MgCl2, 150 mM KCl, 1 mM DTT) containing 125 µM [γ-^{32}P] ATP 20µCi at 30^{o}C for 40 min. The reactions were stopped by 1X Laemmli SDS sample buffer and used for analysis by 10% SDS-PAGE. The radioactive SDS gels were dried and analysed by X-ray Film.

Patch clamp: Cell culture dishes were mounted on the stage of an inverted microscope (IM35, Zeiss) and kept at 37 °C. The bath was perfused continuously with Ringer solution at about 10 ml/min. Patch-clamp experiments were performed in the fast whole-cell configuration. Patch pipettes had an input resistance of 2–4 MΩ, when filled with a solution containing (mM) KCl 30, K-gluconate 95, NaH_2PO_4 1.2, Na_2HPO_4 4.8, EGTA 1, Ca-gluconate 0.758, $MgCl_2$ 1.034, D-glucose 5, ATP 3. pH was 7.2, the Ca^{2+} activity was 0.1 µM. The access conductance was measured continuously and was 60 – 140 nS. Currents (voltage clamp) and voltages (current clamp) were recorded using a patch-clamp amplifier (EPC 7, List Medical Electronics, Darmstadt, Germany), the LH1600 interface and PULSE software (HEKA, Lambrecht, Germany) as well as Chart software (AD-Instruments, Spechbach, Germany). Data were stored continuously on a computer hard disc and were analyzed using PULSE software. In regular intervals, membrane voltages (V_c) were clamped in steps of 10 mV from -50 to +50 mV relative to resting potential. Membrane conductance G_m was calculated from the measured current (I) and V_c values according to Ohm's law.

In vitro transcription and double electrode voltage clamp: cDNAs encoding SK4, hBest1-R218C, hBest1-S358A and hBest1-S358E were linearized and *in vitro* transcribed using T7, T3 or SP6 promotor and polymerase (Promega, USA). 2mg Pak2 enzyme was injected into *Xenopus* oocytes 30min before measurements. Isolation and microinjection of oocytes have been described in details elsewhere[29]. Oocytes were injected with cRNA (10 ng, 47 nl double-

distilled water). Water injected oocytes served as controls. 2 - 4 days after injection, oocytes were impaled with two electrodes (Clark Instruments Ltd, Salisbury, UK), which had a resistances of < 1 MΩ when filled with 2.7 mol/l KCI. Using two bath electrodes and a virtual-ground head stage, the voltage drop across R_{serial} was effectively zero. Membrane currents were measured by voltage clamping (oocyte clamp amplifier, Warner Instruments LLC, Hamden CT) in intervals from -60 to +40 mV (-90 to +30 mV for SK4 expressing oocytes), in steps of 10 mV, each 1 s. The bath was continuously perfused at a rate of 5 ml/min. All experiments were conducted at room temperature (22 °C).

Electron microscopy: For conventional electron microscopy, adult mice were perfusion-fixed for 3 minutes through the distal abdominal aorta with 1x PBS / 2% glutaraldehyde. Tracheas were removed, incubated overnight in fixative and treated with 1% OsO_4 before being embedded in Epon. After ultrathin sections were stained with uranyl acetate and lead citrate, they were analyzed with a Zeiss EM 902 transmission electron microscope equipped with a cooled CCD camera (TRS, Moorenweis, Germany).

To visualize increased Ca^{2+} concentrations in intracellular organelles[30] adult mice were perfusion-fixed for 3 minutes through the distal abdominal aorta with 100 mM sodium cacodylate / 3% paraformaldehyde / 2.5% glutaraldehyde / 50 mM potassium oxalate. Tracheas were removed, incubated overnight in the perfusion buffer and then 3 days in 100 mM sodium cacodylate / 1% OsO_4 / 100 mM potassium ferricyanide before being embedded in Epon. Electron spectroscopic imaging of ultrathin sections was performed in the Zeiss EM 902 transmission electron microscope without further staining. To demonstrate precipitated Ca^{2+} salts, the L2.3 edge at $\Delta E = 346$ eV was used.

Materials and statistical analysis: All compounds (cyclopiazonic acid, ionomycin, ATP, okadaic acid, Pak2-enzyme) were of highest available grade of purity and were from Sigma (Taufkirchen, Germany) or Merck (Darmstadt, Germany). All cell culture reagents were from GIBCO/Invitrogen (Karlsruhe, Germany). The following antibodies were used: mouse anti-hStim1 (Abcam 53551), goat anti-hSK4 (Santa Cruz sc-27081, rabbit anti IP3R-I/II/III (Santa Cruz sc-28613, goat anti hTRPC1 (Santa Cruz sc-15055), rabbit anti-hNa^+/K^+ ATPase (Upstate biotechnology 21217, goat anti hSERCA3 (Santa Cruz sc-8097). Goat anti rabbit IgG –HRP (Acris R1364 HRP), donky anti goat IgG-HRP (Santa Cruz sc 2020) and a mouse anti His-Tag Antibody (Qiagen) were used as a secondary antibodies. Duplexes of 25-nucleotide of RNAi were designed and synthesized by Invitrogen (Paisley, UK). siRNAs for hBest1, xBest2a and xBest2b were: 5´- UGUCCCUGUUGGCUGUGGAUGAGAU-3´, 5´-AUCUGAAUACAUCUCAUCCACAGCC-3´, 5´-GGCGGUGUAAGAUGUUUAACUGGAU-3´. (Student's t-test (for paired or unpaired samples as appropriate) and analysis of variance (ANOVA) was used for statistical analysis. $P<0.05$ was accepted as significant.

F**igure legends**

Fig. 1: Bestrophin 1 controls Ca^{2+} signaling. a) Colocalization of hBest1 and the ER-proteins calnexin and Stim1. b) Coimmunoprecipitation of hBest1 and hStim1 in lysates from HEK293 cells overexpressing both proteins. c) Summary (Mean ± SEM; n=10) of Ca^{2+} transients induced by ATP (10 µM) in hBest1-expressing (red trace) or mock transfected (black trace) HEK293 cells. d) Summary of basal $[Ca^{2+}]_i$ in resting cells and peak $[Ca^{2+}]_i$ after ATP-stimulation in mock transfected and hBest1 expressing cells. e) Recovery rates of $[Ca^{2+}]_i$ after stimulation with ATP in hBest1-expressing or mock transfected HEK293 cells. f) ATP (100 µM) induced Ca^{2+} transients detected with the membrane-bound Ca^{2+} probe FFP-18 in i) mock transfected control cells, ii) hBest1- and iii) hBest1-R218C-expressing cells. g) ATP induced Ca^{2+} transients in the absence of extracellular Ca^{2+}. h) Recovery rates of $[Ca^{2+}]_i$ after stimulation with ATP are reduced in hBest1-R218C expressing HEK293 cells (n = 19 - 32). i) Emptying of ER-Ca^{2+} stores by the SERCA-inhibitor CPA (10 µM) in the absence of extracellular Ca^{2+} in hBest1-expressing or mock transfected HEK293 cells (Mean ± SEM; n=16-27). j) Summaries of the rates for CPA induced Ca^{2+} release (green) and recovery (red). k) ATP-induced oscillations of $[Ca^{2+}]_i$ detected by the Ca^{2+}-probe G-CaMP2 fused to hBest1 (left trace) or hBest1-R218C (right trace), respectively. l) Peak and plateau $[Ca^{2+}]_i$ in hbest1-G-CaMP2 and hbest1-R218C-G-CaMP2 expressing cells (n = 53 - 56). m) *In vitro* phosphorylation of hbest1-C-terminus by Pak2, and lack of phosphorylation in hbest1-R218C. $^{\#}$significant difference when compared to control (unpaired t-test).

Fig. 2: Pak2 phosphorylation of hBest1 activates Ca^{2+} dependent ion currents: a) Whole cell currents in *Xenopus* oocytes expressing $P2Y_2$ receptors (voltage clamped from -60 to +40 mV). ATP (100 µM, black bars) activated endogenous Ca^{2+} dependent Cl^- currents. Injection of Pak2 (2 µg/µl) increased ATP-induced outward and inward currents. b) Concentration-dependent activation of outward currents in the absence (open bars) or presence (black bars)

of Pak2. Removal of extracellular Cl^- (5 mM) inhibited ATP activated whole cell currents. c) Concentration-dependent activation of inward currents. Removal of extracellular Na^+ and Ca^{2+} (0/0 mM) inhibited inward currents (n = 8 – 21). d) ATP activated Cl^- conductances (G_{ATP}) were augmented by injection of Pak2 (2 µg/µl) and exposure to okadaic acid (100 nM), but were inhibited by expression of hBest1-R218C (n = 16 - 38). e) Activation of Cl^- currents by CPA (10 µM) inhibition of SERCA in the absence and presence of Pak2. f) Pak2 augmented CPA-activated Cl^- conductance (n = 9). g) I/V curves from SK4-expressing oocytes. ATP shifted the reversal potential to -90 mV. h) Effect of Pak2 on K^+ currents activated by ATP (10 µM) or ionomycin (1 µM) in oocytes coexpressing $P2Y_2$ receptors and hSK4. i) Pak2 augmented hSK4 whole cell conductance, activated by ATP but not by ionomycin (n = 19 - 22). *significant effect of ATP or ionomycin (paired t-test). $^{\#}$significant difference when compared to absence of Pak2 or control (unpaired t-test). §significant difference when compared to presence of Cl^- or Na^+/Ca^{2+} (unpaired t-test).

Fig. 3: Bestrophin 1 regulates hSK4 and TMEM16A channels: a,b) ATP activated whole cell currents and conductances in *Xenopus* oocytes coexpressing hBest1-R218C, hSK4 and $P2Y_2$-receptors. Activation of hSK4 currents by ATP was reduced (compare Fig. 2i), and was not enhanced by injection of Pak2 enzyme (2 µg/µl) (n = 19 – 22). c) ATP activated whole cell currents in hBest1 expressing HEK293 cells and cells coexpressing Pak2/hBest1, Pak2/siRNA-hBest1, or Pak2/hBest2-R218C. Grey bars indicate partial removal of Cl^- (30Cl) from the extracellular bath solution. d) Whole cell conductances under control conditions, after stimulation of ATP and after partial removal of extracellular Cl^- (30Cl) (n = 9 – 15). e) Endogenous whole cell conductances in human bronchial epithelial cells before and after stimulation with ATP (100 µM). Three different batches of siRNA-Pak2 inhibited ATP-activated conductances (n = 11 – 38). f) Activation of whole cell currents by ATP in control HEK293 cells and after expression of hTMEM16A. g) Summary of the whole cell

conductances in control cells (mock) and after expression of hTMEM16A, hTMEM16A/hBest1 or hTMEM16A/hBest1-R218C (n = 10 – 22). *significant effect of ATP (paired t-test). #significant difference when compared to control (unpaired t-test). §significant difference when compared to hTMEM16A+hBest1 (unpaired t-test).

Fig. 4: a) Electron microscopy images of airway epithelial cells from mBest1-/- and wt animals at low (upper panels; red bar 600 nm) and high magnification (lower panels; red bar 100 nm). EM images revealed swollen ER structures that continue into normal ribosome-occupied ER in mBest1-/- airway cells (arrows). b) Fixation with oxalate containing solutions unmasked electron-dense Ca^{2+}-oxalate deposits in the bloated ER of hBest1-/- airway epithelial cells (arrows). To demonstrate precipitated Ca^{2+} salts, the L2.3 edge at $\Delta E = 346$ eV was used (lower panels). Bright color indicates precipitates with high Ca^{2+} concentration in the ER of cells from mBest1-/- mice (arrow at right lower image).

Fig.1

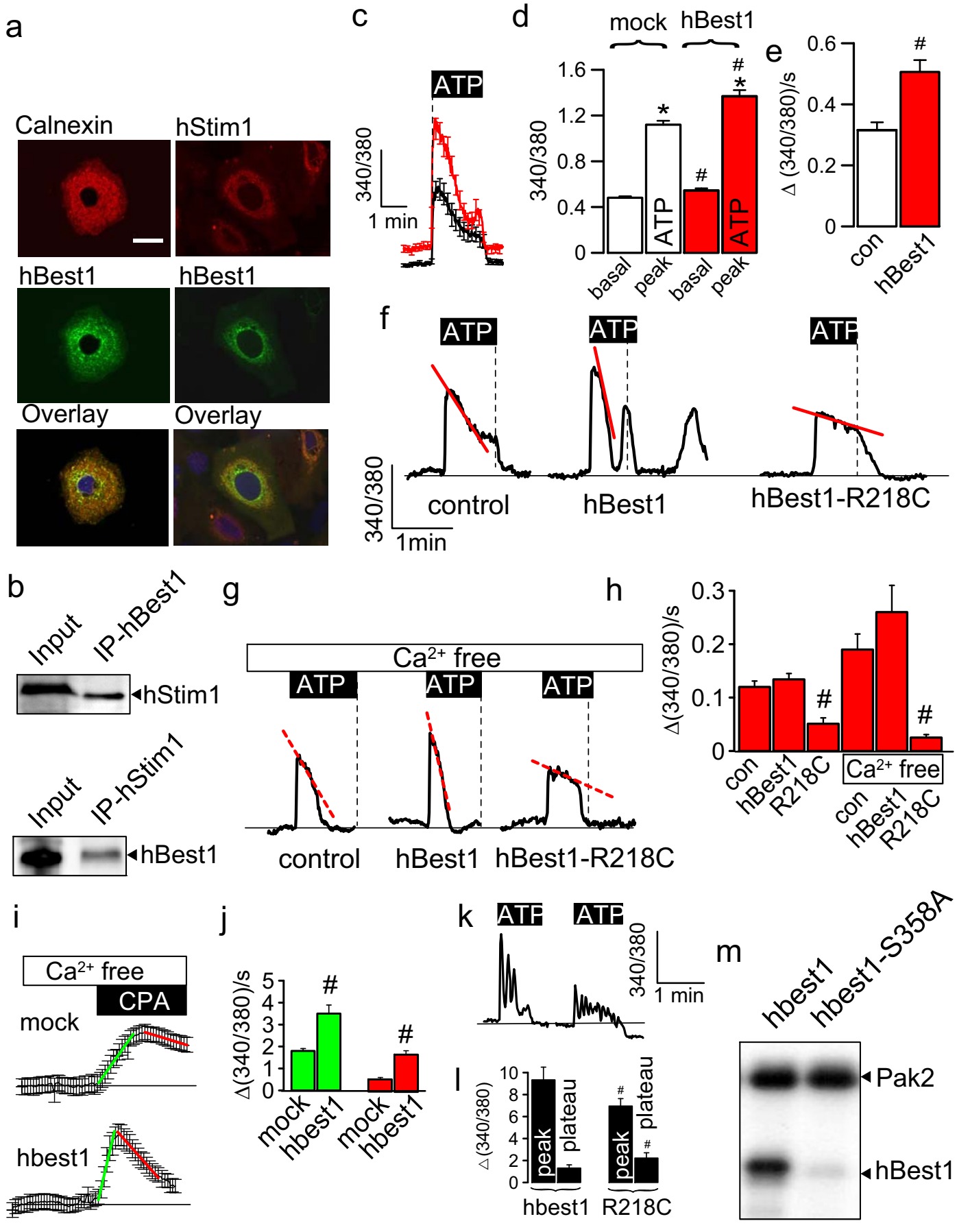
a
Calnexin
hStim1
hBest1
hBest1
Overlay
Overlay
c
ATP
340/380
1 min
d
mock
hBest1
1.6
1.2
0.8
0.4
0
340/380
ATP
ATP
basal
peak
basal
peak
e
0.6
0.4
0.2
0
Δ (340/380)/s
con
hBest1
f
ATP
ATP
ATP
340/380
1min
control
hBest1
hBest1-R218C
b
Input
IP-hBest1
hStim1
Input
IP-hStim1
hBest1
g
Ca2+ free
ATP
ATP
ATP
control
hBest1
hBest1-R218C
h
0.3
0.2
0.1
0
Δ(340/380)/s
con
hBest1
R218C
Ca2+ free
con
hBest1
R218C
i
Ca2+ free
CPA
mock
hbest1
j
5
4
3
2
1
0
Δ(340/380)/s
mock
hbest1
mock
hbest1
k
ATP
ATP
340/380
1 min
l
10
8
6
4
2
0
Δ(340/380)
peak
plateau
peak
plateau
hbest1
R218C
m
hbest1
hbest1-S358A
Pak2
hBest1

Fig. 2

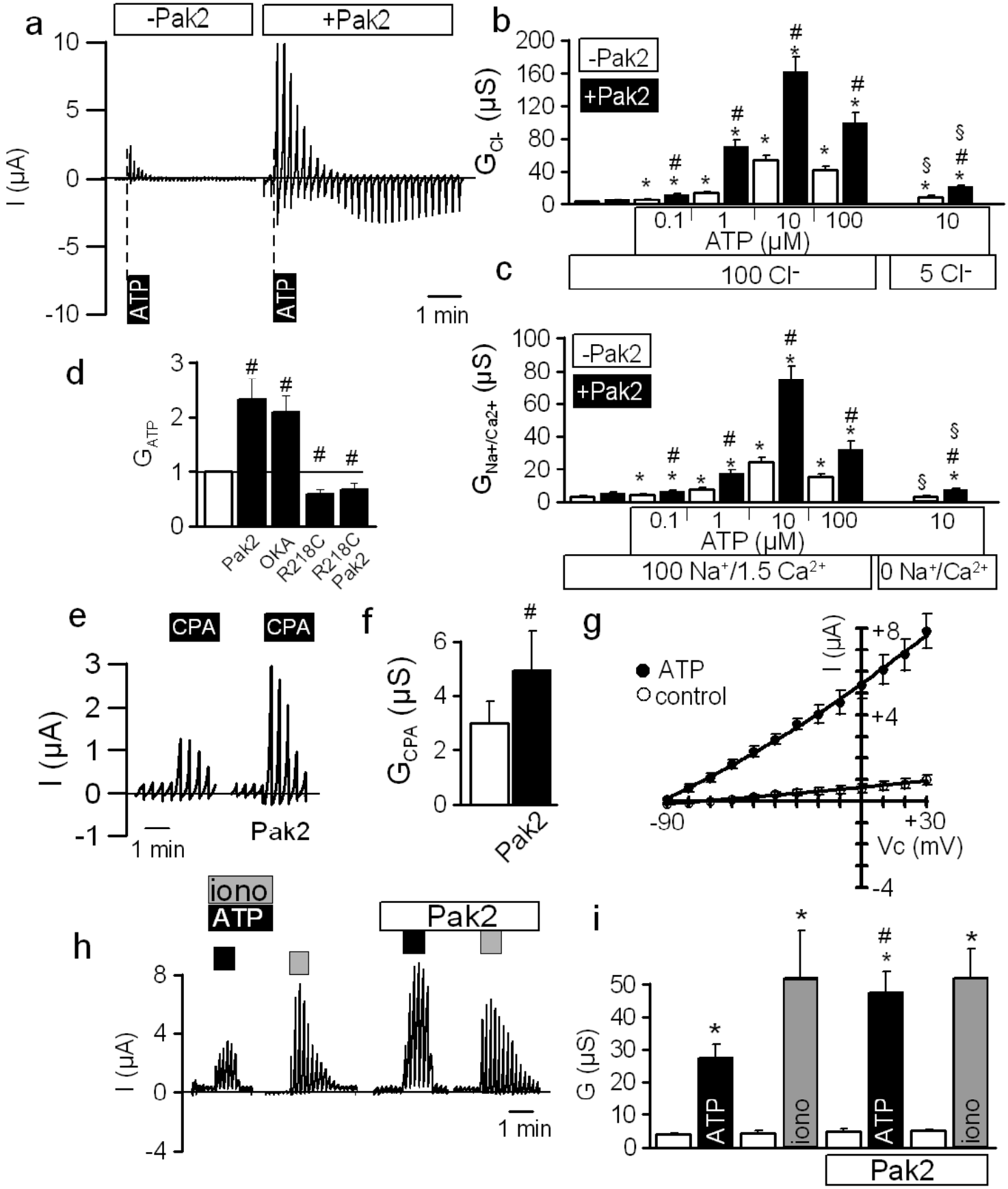
a
-Pak2
+Pak2
I (μA)
ATP
ATP
1 min
b
-Pak2
+Pak2
G_{Cl-} (μS)
0.1
1
10
100
10
ATP (μM)
100 Cl-
5 Cl-
c
$G_{Na+/Ca2+}$ (μS)
-Pak2
+Pak2
0.1
1
10
100
10
ATP (μM)
100 Na+/1.5 Ca2+
0 Na+/Ca2+
d
G_{ATP}
Pak2
OKA
R218C
R218C
Pak2
e
CPA
CPA
I (μA)
1 min
Pak2
f
G_{CPA} (μS)
Pak2
g
ATP
control
I (μA)
+8
+4
-4
-90
+30
Vc (mV)
h
iono
ATP
Pak2
I (μA)
1 min
i
G (μS)
ATP
iono
ATP
iono
Pak2

Fig. 3

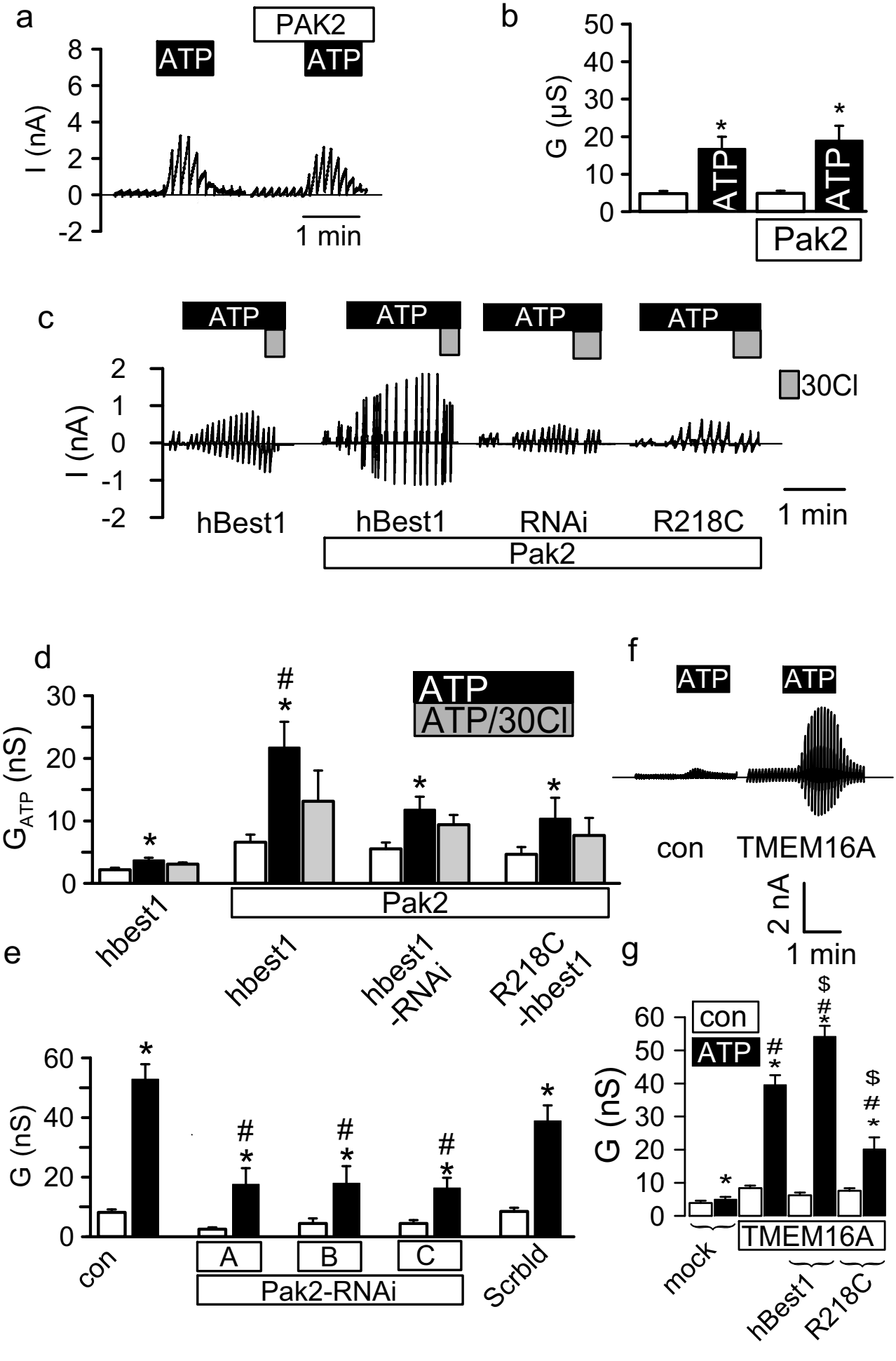
a
PAK2
ATP
ATP
I (nA)
8
6
4
2
0
-2
1 min
b
G (μS)
50
40
30
20
10
0
ATP
ATP
Pak2
c
ATP
ATP
ATP
ATP
30Cl
I (nA)
2
1
0
-1
-2
hBest1
hBest1
RNAi
R218C
1 min
Pak2
d
ATP
ATP/30Cl
G_{ATP} (nS)
30
20
10
0
hbest1
Pak2
e
hbest1
hbest1
-RNAi
R218C
-hbest1
G (nS)
60
40
20
0
con
A
B
C
Scrbld
Pak2-RNAi
f
ATP
ATP
con
TMEM16A
2 nA
1 min
g
G (nS)
60
50
40
30
20
10
0
con
ATP
mock
TMEM16A
hBest1
R218C

Fig. 4